Anal. Chem. **2000,** *72,* 5549−5555

Spectroelectrochemical Sensing Based on Multimode Selectivity Simultaneously Achievable in a Single Device. 9. Incorporation of Planar Waveguide Technology

Susan E. Ross, Carl J. Seliskar,* and William R. Heineman*

Department of Chemistry, University of Cincinnati, P.O. Box 210172, Cincinnati, Ohio 45221-0172

Incorporation of planar waveguide technology into a spectroelectrochemical sensor is described. In this sensor design, a potassium ion-exchanged BK7 glass waveguide was over-coated with a thin film of indium tin oxide (ITO) that served as an optically transparent electrode. A chemically selective film was spin-coated on top of the ITO film. The sensor supported five optical modes at 442 nm and three at 633 nm. Investigations on the impact of the ITO film on the optical properties of the waveguide and on the spectroelectrochemical performance of the sensor are reported. Sensing was based on the change in attenuation of light propagated through the waveguide resulting from an optically absorbing analyte. By applying either a triangular or square wave excitation potential waveform, electromodulation of the optical signal has been demonstrated with $Fe(CN)_6^{3-/4-}$ as a model electroactive couple that partitions into a PDMDAAC−SiO_2 film {where PDMDAAC = poly(dimethyldiallylammonium chloride)} and absorbs at 442 nm.

Recently, a new sensor concept based on three modes of selectivity (chemical partitioning, electrochemistry, spectroscopy) has been demonstrated.[1−7] In this concept, 3-fold selectivity for the analyte by the sensor was obtained by incorporation of a chemically selective film, choice of the electrode potential, and choice of the wavelength of the light. The concept has been successfully demonstrated using a prototype multiple internal reflection (MIR) optic, which consisted of a simple bilayer of an indium tin oxide (ITO) optically transparent electrode (OTE) deposited on a 1-mm-thick glass substrate. Analyte detection was enhanced by overcoating the ITO-coated optic with a chemically selective film and was based on the change in the attenuation of light guided through the sensor.

An important extension of our work was to develop a planar waveguide to replace the MIR optic. The potential advantages of waveguides[8−10] over MIR devices are several: (1) increased sensitivity and better detection limits due to higher density of reflections; (2) greater versatility in choice of optical designs, including more sophisticated configurations, such as Mach Zehnder interferometers; and (3) the ability to micromachine sensors in complex platforms. The uses of waveguides for chemical sensing have been amply reported in the literature.[9,10] Previously reported types of planar waveguide chemical sensors include channel[11−14] and slab (or planar)[15−17] designs and Mach Zehnder interferometers.[18−20]

There have been several reports of waveguide designs for spectroelectrochemical sensing. Itoh and Fujishima[16] demonstrated that a multimode slab waveguide, made by potassium ion exchange and covered by a thin conducting layer of antimony-doped tin oxide, could function as both an electrode and an optical sensor for methylene blue. They later developed a single-mode potassium ion-exchanged waveguide for ammonia sensing.[17] Another sensor, developed by Piraud and co-workers,[12,13] was for chlorine. More recently, the work of Dunphy and co-workers[15] provided conclusive evidence of the large sensitivity enhancements possible with waveguide sensing of methylene blue at an electrode

(1) Shi, Y.; Slaterbeck, A. F.; Seliskar, C. J.; Heineman, W. R. *Anal. Chem*. **1997**, *69*, 3679−3686.
(2) Shi, Y.; Seliskar, C. J.; Heineman, W. R. *Anal. Chem*. **1997**, *69*, 4819−4827.
(3) Slaterbeck, A. F.; Heineman, W. R.; Ridgway, T. H.; Seliskar, C. J. *Anal. Chem*. **1999**, *71*, 1196−1203.
(4) Gao, L.; Seliskar, C. J.; Heineman, W. R. *Anal. Chem*. **1999**, *71*, 4061−4068.
(5) Hu, Z.; Slaterbeck, A. F.; Seliskar, C. J.; Ridgway, T. H.; Heineman, W. R. *Langmuir* **1999**, *15*, 767−773.
(6) Slaterbeck, A. F.; Stegemiller, M. L.; Heineman, W. R.; Ridgway, T. H.; Seliskar, C. J. *Anal. Chem*., in press. (ac991460h)
(7) DiVirgilio-Thomas, J.; Seliskar, C. J.; Heineman, W. R. *Anal. Chem*. **2000**, *72*, 3461−3467.
(8) Mendes, S. B.; Saavedra, S. S. *Appl. Opt.* **2000**, *39*, 612−621.
(9) Plowman, T. E.; Saavedra, S. S.; Reichert, W. M. *Biomaterials* **1998**, *19*, 341−355.
(10) Lukosz, W. *Sens. Actuators B* **1995**, *29*, 37−50.
(11) Klein R.; Voges, E. *Sens. Actuators B* **1993**, *11*, 221−225.
(12) Piraud, C.; Mwarania, E.; Wylangowski, G.; Wilkinson, J.; O'Dwyer K.; Schiffrin, D. J. *Anal. Chem*. **1992**, *64*, 651−655.
(13) Piraud, C.; Mwarania, E. K.; Yao, J.; O'Dwyer, K.; Schiffrin, D. J.; Wilkinson, J. S. *J. Lightwave Technol.* **1992**, *10*, 693−699.
(14) Ross, S. E.; Slaterbeck, A. F.; Shi, Y.; Aryal, S.; Maizels, M.; Seliskar, C. J.; Heineman, W. R.; Ridgway, T. H.; Nevin., J. H. *Proc. SPIE-Int. Soc. Opt. Eng.* **1999**, *3259*, 268−279.
(15) Dunphy, D. R.; Mendes, S. B.; Saavedra S. S.; Armstrong, N. R. *Anal. Chem*. **1997**, *69*, 3086−94.
(16) Itoh, K.; Fujishima, A. In *Electrochemistry in Transitions*; Murphy, O. J., Ed; Plenum Press: New York, 1992; pp 7043−7045.
(17) Itoh, K.; Fujishima, A. *J. Phys. Chem*. **1988**, *92*, 7043−7045.
(18) Schipper, E. F.; Rauchalles, S.; Kooyman, R. P. H.; Hock, B.; Greve, J. *Anal. Chem*. **1998**, *70*, 1192−1197.
(19) Gauglitz, G.; Ingenhoff, J. *Sens. Actuators B* **1993**, *11*, 207−212.
(20) Helmers, H.; Greco, P.; Rustad, R.; Kherrat, R.; Bouvier, G.; Benech, P. *Appl. Opt*. **1996**, *35*, 676−680.

10.1021/ac0007736 CCC: $19.00 © 2000 American Chemical Society
Published on Web 10/21/2000

surface using a single-mode slab waveguide coated by a silica buffer layer topped with a thin conducting film of ITO.

A goal of this work was to fabricate a prototype planar waveguide spectroelectrochemical sensor and to compare it to our previously reported MIR devices. In this paper, we demonstrate the essential process of electromodulation using an ITO-coated, ion-exchanged BK7 glass waveguide (ITO IEBK7), overcoated with a sol−gel processed anion-selective film. We also report the use of near-UV (442 nm) wavelength light and the resulting waveguide mode structure. Fabrication of the sensor, and the spectroscopic and electrochemical effects of the ITO layer in particular, are discussed.

EXPERIMENTAL SECTION

Chemicals. The following chemicals were used for spectroelectrochemistry: potassium nitrate (Fisher Scientific), potassium ferrocyanide (Aldrich), tetraethoxysilane (TEOS; Aldrich), and poly(dimethyldiallylammonium chloride) (PDMDAAC; Polysciences, 20 wt % aqueous solution, 200 000−350 000 MW). All reagent solutions were made by dissolving the appropriate amounts of chemicals in 0.1 M potassium nitrate solution (prepared with deionized water from a Barnstead water purification system). All reagents were used without further purification. BK7 plates (1.0 in. × 1.0 in. × 0.062 in.) were purchased from Esco Products and cut to size as needed.

Fabrication of ITO IEBK7 Waveguides. BK7 plates were first cleaned with Alconox and rinsed with isopropyl alcohol and then with deionized water. For ion exchange, several plates were placed in a large crucible containing KNO_3 and then in an oven, which was heated to 390 °C and held at that temperature for 8 h. After ion exchange, the individual pieces were quickly lifted out of the hot liquid KNO_3 and cooled on a wire mesh with a subsequent deionized water rinse to remove residual salt. The change in refractive index, Δn, and the diffusion depth of the ion-exchanged BK7 were estimated from published diffusion coefficients and from extrapolation of published curves of Δn versus time (vide infra). For refractive indices of the ion-exchanged waveguide layer, a Δn of 0.008 was added to the BK7 substrate refractive index at both 442- and 633-nm wavelengths. Electron beam deposition of ITO onto a large cassette of individual waveguide pieces was done by General Vacuum (Cleveland, OH). Refractive index values for the ITO films were determined using a Woollam variable-angle spectroscopic ellipsometer. ITO film resistances were measured on 1.27 cm × 2.54 cm coated pieces of IEBK7; values were found to be between 100 Ω and 7 kΩ across the 2.54-cm length. Resistance values varied depending on the location of the waveguides on the ITO coating cassette. Only ITO waveguides with resistance values less than 1 kΩ were employed.[21]

Preparation of PDMDAAC−SiO_2 Films. Silica sol stock solutions were prepared according to a previously reported protocol.[22] Film thickness was estimated by using the optical interference method[22,23] on films made under identical conditions on soda lime glass. Prior to use, the films were rehydrated in supporting electrolyte solution for at least 8 h. The refractive index of the hydrated films was estimated to be 1.39, based on an average value between water ($n \approx 1.33$) and the dry film ($n \approx 1.46$),[22] and on n values for similar SiO_2−composite films.[24]

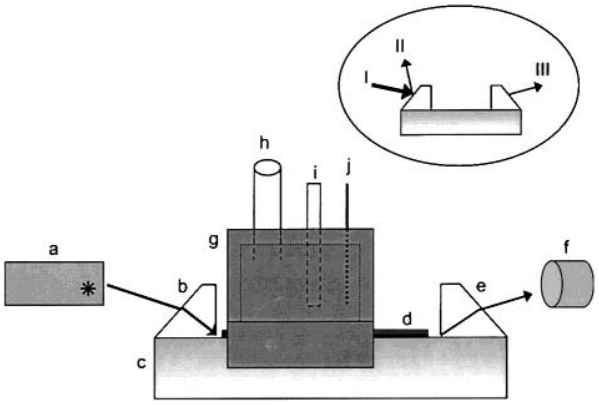

Figure 1. Schematic of the sensor instrumentation for electromodulation and mode evaluation. Key: (a) laser (HeCd or HeNe); (b) SF6 prism; (c) ion-exchanged BK7 waveguide; (d) thin ITO layer; (e) SF6 prism; (f) detector (PMT or power monitor); (g) sample cell; (h) sample inlet tubing; (i) Ag/AgCl reference electrode; (j) Pt auxiliary electrode. The inset shows a diagram of the positions where power measurements were made for the power loss study. The positions correspond to the following: I, laser directly; II, back-reflection of the first prism face; III, exit prism.

Instrumentation. A diagram of the instrumentation is shown in Figure 1. A 25-mW TEM_{00} 441.6-nm HeCd laser (Kimmon Electric, model IK4153R-C) and a 10-mW TEM_{00} 632.8-nm HeNe laser (Newport, model 3225H-PC) served as light sources. The waveguide sensor was mounted on a high-resolution rotation stage (Klinger; 0.5° resolution). Laser light was directly coupled in to and out of the waveguide using two SF6 coupling prisms (Karl Lambrecht). Pressure was lightly applied to hold the first prism (b, Figure 1) in place. The second prism (e, Figure 1) was fixed with Meltmount. The bottom waveguide surface was blackened to reduce base-glass multiple internal reflection of light that was prism coupled into the optic.

In the attenuation study, the polarization of HeCd laser light was rotated from TE to TM using a Babinet Soleil compensator (Karl Lambrecht). HeNe laser light polarization was rotated by simply turning the cylindrical head. The optical power was measured at three positions, as shown in the inset of Figure 1, using a power meter (Kimmon Electric, model PM-300). The attenuation, in percent power (% P), at either position II or III was calculated relative to that measured at position I. All % P data were converted to decibels per centimeter (of ITO) units (path length 1.7 cm) and averaged over four waveguides for each wavelength.

For electromodulation experiments, light from the exit prism (e, Figure 1) was directed to a phototube (Hamamatsu R955) and the output voltage digitized and stored. Electrochemistry was performed using a BAS CV27 potentiostat or a simple three-op-amp potentiostat built in our laboratory.[3] The reference electrode was Ag/AgCl, 3 M KCl (Cypress Systems, model EE008); the auxiliary electrode was platinum wire. A syringe was used to make all sample introductions to the cell. *Sensor absorbance* was defined as $A = \log(I_o/I)$, where I_o was the light intensity propagated through the waveguide in supporting electrolyte and I was the light intensity under sample-loaded conditions.

Experimental Protocols. The concentration study was performed by first determining an optical baseline in supporting

(21) Luff, J.; Wilkinson, J. S.; Perrone, G. *Appl. Opt.* **1997**, *36*, 7066−7072.
(22) Shi, Y.; Seliskar, C. J. *Chem. Mater.* **1997**, *9*, 821−829.
(23) Goodman, A. M. *Appl. Opt.* **1978**, *17*, 2779−2786.
(24) Clager, M. R., unpublished results.

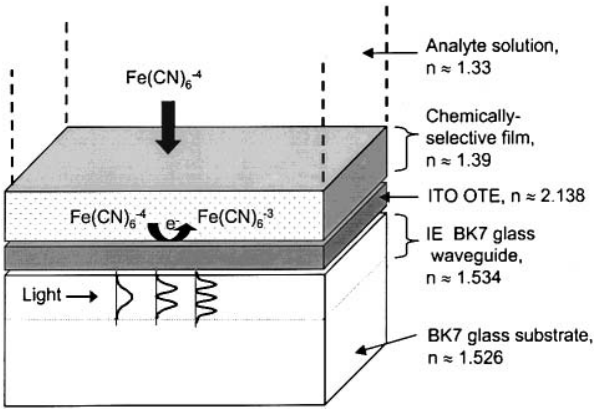

Figure 2. A cross section of the ITO IEBK7 sensor. The optical layers are labeled with refractive indices at 442 nm.

electrolyte at −0.80 V. The method of successive additions was used to determine a concentration curve. Prior to injecting 5 mL of the analyte standard solution, the cell was flushed with 20 mL of supporting electrolyte (open circuit) for 1 min. Then 5 min after injection, a CV was obtained at 10 mV/s, followed by a double-potential step (~3 min/step). Average values of the maximum absorbance were calculated from the last 30 digitized values recorded preceding the first cathodic step.

RESULTS AND DISCUSSION

Description of the ITO IEBK7 Waveguide. We purposely chose and fabricated a multimode waveguide for sensing.[11,25] The optical configuration of the corresponding sensor and the sample, illustrated in Figure 2, is a five-layer structure based on a K^+–Na^+ ion-exchanged BK7 glass substrate. The ion-exchanged layer is a graded-index layer with the refractive index assumed to be highest at the surface and decreasing to the substrate value in the glass interior. Above the graded-index BK7 region is a thin (~150 nm) conducting layer of ITO that serves as the OTE. A sol–gel processed silica composite with PDMDAAC forms the topmost layer of the sensor structure and acts as a selective film for concentrating the analyte (ferrocyanide). The external solution layer (sample) is the top layer and is typically aqueous.

Characterization of the waveguide included estimation of the parameters Δn, the change in the refractive index at the waveguide surface, and d, the ion-exchange depth, so that the number of waveguide modes could be predicted and compared with experiment. For ion-exchanged waveguides, determination of Δn and d is complicated by the graded-index profile created by the ion-exchange process.[26–32] Experimentally, the refractive index profile can be controlled only by ion-exchange temperature and time.[28] One approach to estimate the waveguide parameters Δn and d has been to develop mathematical models of the index profile based on the diffusional boundary conditions, ion properties (e.g., polarizability, radius), ion concentration, temperature, and time.[27–33] Typically, the Wentzel–Kramers–Brillouin (WKB) or the inverse WKB dispersion relationship, in conjunction with a selected profile model, is used[28–31] to determine Δn ($\Delta n = \Delta n_{surface} - \Delta n_{substrate}$).

For our prototype waveguide, an estimation of Δn and d was deemed sufficient for initial characterization. Our approach was to employ a simple effective step-index profile model, rather than the more complex graded-index profile, to predict the number of modes. The mode calculation began by estimating Δn and depth values from previous work on BK7 glass.[28–30] The Δn value for our waveguide was obtained by extrapolation of the theoretical Δn values at 633 nm reported by Ciminelli et al. (Figure 1b, ref. 29) and by Gortych and Hall (Figures 1 and 3, ref 30); Δn was estimated to be 0.008. The Einstein–Smolechowski equation was employed to approximate δ,

$$\delta = \sqrt{2Dt} \qquad (1)$$

since a linear relationship between $\sqrt{t}$ and δ has been well established for ion-exchanged waveguides.[29–31] For the range of diffusion coefficients reported in the literature (1.60–5.11 $\mu m^2/h$),[30,31] and the time, t, of 8.0 h, our calculated δ values were found to vary from 5.1 to 9.0 μm. The apparent agreement of these δ values with the results of more complex models[28–30] (δ = 5.9[30]–11.7 μm[29]) is surprisingly good.

With Δn and δ estimated, the number of waveguide supported modes, $m + 1$ (the fundamental mode is $m = 0$), can be estimated using a step-index model and

$$m = [2d(n_w^2 - n_s^2)^{1/2}]/\lambda \qquad (2)$$

where the effective depth δ is substituted for the step-index depth, d, and the other variables are as follows: n_w and n_s, the refractive indices of the waveguide ($n_{442\ nm} = 1.534$; $n_{633\ nm} = 1.523$) and of the glass substrate ($n_{442\ nm} = 1.526$; $n_{633\ nm} = 1.515$), respectively, and, λ, wavelength. Using the average effective depth, $\delta_{av} = 7.1$ μm determined from eq 1, the predicted number of modes, $m + 1$, was six at 442 nm and four at 633 nm.

The experimental value for the number of modes was determined using the M-line technique.[32,33] The M-lines, each corresponding to one waveguide mode, were visually identified as five at 442 nm and three at 633 nm. The observed ratio of five (442 nm) to three (633 nm) mode lines was similar to the theoretical ratio (six to four), indicating that our effective step-index model provided a reasonable estimate.

ITO Optical Constants, *n* and *k*. The complex refractive index and resistance of an ITO film depend on the chemical composition and deposition process[21,34–36] and have a major impact on the optical [21,34–39] and electrochemical[34,40] performance of this semiconductor. Since we had fabricated a device with a nonstand-

(25) Saavedra, S. S.; Reichert, W. M. *Anal. Chem.* **1990**, *62*, 2251–2256.
(26) Doremus, R. H. *J. Phys. Chem.* **1964**, *68*, 2212–2219.
(27) Findakly, T. *Opt. Eng.* **1985**, *24*, 244–250.
(28) Opilski, A.; Rogozinski, R.; Blahut, M.; Karasinski, P.; Gut, K.; Opilski, Z. *Opt. Eng.* **1997**, *36*, 1625–1638.
(29) Ciminelli, C.; D'Orazio, A.; De Sario, M.; Gerardi, C.; Petruzzelli, V.; Prudenzano, F. *Appl. Opt.* **1998**, *37*, 2346–2356.
(30) Gortych, J. E.; Hall, D. G. *IEEE J. Quantum Electron.* **1986**, *QE–22*, 892–895.
(31) Yip, G. L.; Albert, J. *Opt. Lett.* **1985**, *10*, 151–153.
(32) Tamir, T. In *Integrated Optics*; Tamir, T., Ed.; Topics in Applied Physics 7; Springer-Verlag: New York, 1975; Chapter 3.
(33) Tien, P. K. *Appl. Opt.* **1971**, *10*, 2395–2413.
(34) Chopra, K.; Major, S.; Pandya, K. *Thin Solid Films* **1983**, *102*, 1–46.
(35) Manivannan, P.; Subrahmanyan, A. *J. Phys. D: Appl. Phys.* **1993**, *26*, 1510–1515.
(36) Tahar, R. B. H.; Ban, T.; Ohya, Y.; Takahashi, Y. *J. Appl. Phys.* **1998**, *83*, 2631–2645.

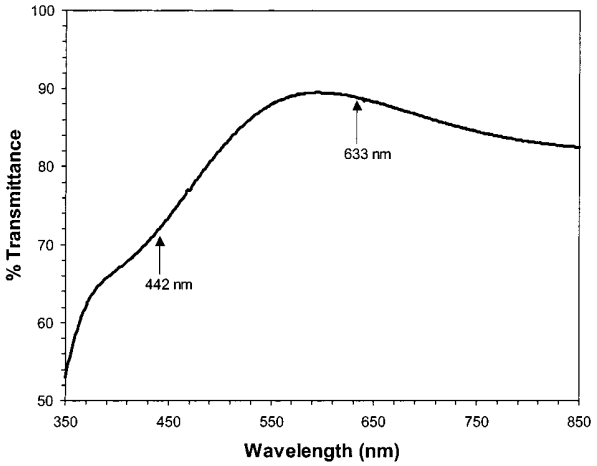

Figure 3. Transmittance spectrum of an ITO IEBK7 waveguide (single-pass, normal incidence, air blank). The wavelengths of the laser line sources used are indicated by vertical lines.

ard ITO transparent electrode, it was important to characterize this sensor component. The real part of the refractive index, *n*, and the imaginary part, *k* (extinction coefficient), were studied by variable-angle spectroscopic ellipsometry.[41] The *n* values for the ITO film were found to be 2.138 and 1.927 at 442 and 633 nm, respectively. These *n* values are significantly higher than 1.78−1.85 at 633 nm reported by Woollam and co-workers[42] and Luff et al.[21] but similar to those reported by Synowicki[43] and Nagatomo et al.[44] The extinction coefficient *k* was found to be 0.029 and 0.009 at 442 and 633 nm, respectively, and these values are consistent with the published values of 0.03 or less.[21,43]

Figure 3 shows a transmittance spectrum of the ITO film taken at normal incidence and it is similar to those of Luff et al. (95 nm thick),[21] Manivannan and Sabrahmanyan (200−300 nm thick),[35] and Karawasa and Miyata (115 nm thick),[45] given the differences in film thickness. In reported work,[35,44,45] an increase in the % *T* observed in the wavelength region 350−400 nm has been attributed to In_2O_3. The absence of this pronounced feature in Figure 3 suggests that the In_2O_3 concentration in our ITO is lower, possibly due to an increased tin dopant concentration[35,44] or a decrease in oxygen concentration.[36,45] In either case, the likely result is an increase in the free carrier concentration of the semiconductor and a higher refractive index for our ITO. An increase in the free carrier concentration *N* leads to an increase in the optical absorption[15,34,44,45] by the semiconductor itself. The free carrier absorption in the visible wavelength region is given by

$$A_{fc} = \lambda^2 e^3 N l / 4\pi^2 \epsilon_o c^3 n m^{*2} \mu \qquad (3)$$

where λ is the wavelength, *e* is the electron charge, *l* is the optical path length, ϵ_o is the dielectric constant of ITO, *c* is the velocity of light, *m** is the reduced mass of the electron, and μ is the carrier mobility. Consequently, significant optical attenuation due to an increased A_{fc} was expected for our ITO-coated waveguide.

Table 1. Power Attenuation of IEBK7 Waveguides with and without ITO Film

	power attenuation[a] (dB/cm) at λ given	
	442 nm	633 nm
no ITO	(TE) 5 ± 2	(TE) 4 ± 2
no ITO	(TM) 4 ± 1	(TM) 4 ± 1
ITO	(TE) 10 ± 4	(TE) 8 ± 2
ITO	(TM) 8 ± 2	(TM) 6 ± 1

[a] Average attenuation values; standard deviations (1σ) were calculated for four waveguides.

Waveguide Attenuation Study. The high real part of the refractive index (*n*) and the extinction coefficient (*k*) of ITO limit[12,13,15,16,21,46] the possible configurations for a sensor. In our sensor design (Figure 2), the placement of and thickness of the ITO layer directly on the waveguide were imposed by our own limited fabrication capabilities and our ITO supplier constraints. Since optical throughput was important to the success of the spectroelectrochemical waveguide sensor, we undertook a characterization of the impact of ITO on the optical loss of the sensor.

Table 1 summarizes the waveguide attenuations at 442 and 633 nm for four devices. The first source of power loss (see Figure 1, inset) was due to the reflection of the laser beam from the first prism face. At 442 nm, the measured amount of power reflected relative to the incident laser power was 5 (TE) and 8% (TM); at 633 nm, 8 (TE) and 10% (TM). The amount of power reflected can be calculated from the Fresnel relationships for TE or TM polarized incident light using the appropriate optical constants. The experimental measurements agree reasonably well with the theoretical % *P* values of 7 (TE) and 11% (TM) at 442 nm, and 5 (TE) and 11% (TM) at 633 nm. From these results, it is clear that this source of loss is relatively minor.

Several trends in the waveguide attenuation values can be seen in Table 1. First, the standard deviations of the measurements were relatively large (∼±2 dB/cm) and arose principally from the poor reproducibility of prism coupling.[32,33,47] Second, TM-polarized light coupled better than TE, an observation that has been reported by others.[13,21] Third, the attenuation was much greater with ITO-coated waveguides. Additionally, the differences in the extinction coefficient of ITO ($k_{442\ nm} = 0.029$; $k_{633\ nm} = 0.009$) with wavelength are consistent with the observed trend in the attenuations at 442 and 633 nm. Fourth, the attenuation values for the ion-exchanged BK7 waveguides (no ITO) were remarkably high (4−5 dB/cm). In comparison, Ciminelli et al.[29] reported losses of ∼0.51 dB/cm or less for their waveguide (633 nm). Our observed values suggest inefficient prism coupling as the major source of these losses. Fifth, the placement of the ITO layer directly on the waveguide without a buffer layer resulted in

(37) Reed, A. H.; Yeager, E. *Electrochim. Acta* **1970**, *15*, 1345−1354.
(38) Rothenberger, G.; Fitzmaurice, D.; Gratzel, M. *J. Phys. Chem.* **1992**, *96*, 5983−5986.
(39) Winograd, N.; Kuwana, T. *J. Electroanal. Chem.* **1969**, *23*, 333−42.
(40) Martinez, M. A.; Herrero, J.; Gutierrez M. T. *Electrochim. Acta* **1992**, *37*, 2565−2571 and references therein.
(41) Zudans, I., unpublished results.
(42) Woollam, J. A.; McGahan, W. A.; Johs, B. *Thin Solid Films* **1994**, *241*, 44−46.
(43) Synowicki, R. A. *Thin Solid Films* **1998**, *313−314*, 394−397.
(44) Nagatomo, T.; Maruta, Y.; Omoto, O. *Thin Solid Films* **1990**, *192*, 17−25.
(45) Karawasa, T.; Miyata, *Thin Solid Films* **1993**, *223*, 135−139.
(46) Srinivasan, V. S.; Kuwana, T. *J. Phys. Chem.* **1968**, *78*, 1144−48.
(47) Weber, H. P.; Dunn, F. A.; Leibolt, W. N. *Appl. Opt.* **1973**, *12*, 755−757.

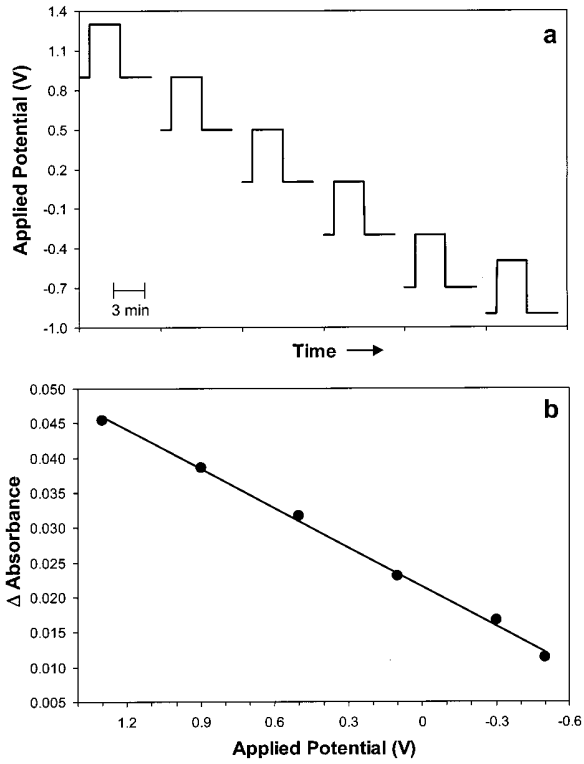

Figure 4. Potential dependence on modulated absorbance for sensor consisting of a PDMDAAC−SiO_2-coated ITO IEBK7 waveguide equilibrated in supporting electrolyte (0.1 M KNO_3). (a) The potential waveform applied to ITO. For each cycle, the initial potential was held for 1 min, then stepped 400 mV more positive. and held for 3 min. The return step potential (initial) was held for another 3 min. Initial potentials were +0.90, +0.50, +0.10, −0.30, −0.70, and −0.90 V. Between each cycle, no potential was applied, as denoted by the breaks along the time axis. (b) The ΔA values shown are the differences in absorbances at each potential limit for each cycle. R^2 = 0.997 for the linear fit. E (V) vs Ag/AgCl; λ = 442 nm.

reducing the power throughput by 2−4 dB/cm. However, the magnitude of our losses is smaller than the losses of ∼4 dB/cm reported by Luff and co-workers[21] for a 50-nm-thick ITO film and of 4−7 dB/cm (depending on mode) for a 100-nm-thick SnO_2 film by Itoh and Fujishima[16] at 633 nm. The differences between our measurements and those reported might, in part, be ascribed to a compromised coupling to our waveguides and the support of some MIR within the substrate that would contaminate the optical throughput yielding low loss values. Nonetheless, our observed attenuation values clearly confirm the major power loss due to ITO directly applied to the waveguide.

Electromodulation of ITO. It is known that the optical properties of ITO are affected by imposing an electrical potential on this semiconductor. We, therefore, examined the behavior of ITO films with potential steps at different regions of the potential window. A series of six double-step potential cycles (Figure 4a) was applied to a PDMDAAC−SiO_2-coated ITO IEBK7 waveguide that had been equilibrated in supporting electrolyte. The potential range examined (+1.30 to −0.90 V) spans the useful potential range of ITO. The changes in sensor absorbance, ΔA, for each potential cycle are shown in Figure 4b. The largest ΔA value of 0.045 was obtained at the most positive potential (step: +0.90 to +1.30 V), and ΔA in other cycles decreased linearly as the potential became more negative. This trend has been reported by others,[17,37,39] and the magnitudes of our results are consistent with reported values[38,46] for other semiconductor electrodes. Such an absorbance change has been explained by the increased free carrier absorption, which in turn depends on the applied potential. The potential-dependence of absorption has been rationalized as a double-layer phenomenon in several reports by Reed and Yeager,[37] Rothenberger and co-workers,[38] and Kuwana,[39,46] and co-workers. Another possibility is that the modulation might, at least in part, be caused by the refractive index of the electrode varying with potential. Several studies[14,34,46] have shown, however, that the contribution from such a variation is negligible. The net result of our measurements is that there is an inherently large optical absorbance change in our ITO to be expected as the potential is cycled in electromodulation experiments and that this change scales linearly with applied potential.

Electromodulation of Ferrocyanide. The ferri/ferrocyanide couple, $Fe(CN)_6^{3-/4-}$, was chosen as a benchmark with which to demonstrate electromodulation of an analyte that partitions into a selective film on the waveguide sensor. The chemically selective film, PDMDAAC−SiO_2, has been shown to be well-suited for sensors for ferri/ferrocyanide.[1,22,48,49] The chosen redox couple has well-defined electrochemistry that is accompanied by distinct spectral changes in the visible wavelength region (380−450 nm). At reducing potentials ($E^{\circ\prime}$ = +0.25 V vs Ag/AgCl), ferrocyanide, $Fe(CN)_6^{4-}$, is colorless and has essentially no absorbance at the 442-nm HeCd laser line. At more positive potentials, ferricyanide, $Fe(CN)_6^{3-}$, is colored and absorbs moderately at 442 nm ($\epsilon \approx$ 503 M^{-1} cm^{-1}). With either suitably chosen triangular or square wave excitation potentials applied, the partitioned analyte will cycle between its reduced and oxidized states, resulting in the modulation of waveguide propagated 442-nm light.[1,6]

Initially, a scan rate experiment was conducted to characterize the electrochemistry within the selective film and the ITO electrode properties. Figure 5a shows the CVs recorded at scan rates from 2 to 500 mV/s with a preloaded PDMDAAC−SiO_2-coated ITO IEBK7 waveguide. Linear plots (not shown) of peak currents, i_{pc} and i_{pa} versus the square root of the scan rate, $\sqrt{v}$, indicated that the electrochemistry in the film was diffusion-controlled, typical for a relatively thick polymer film (∼650-nm thickness).[1,4,49]

The scan rate had a significant effect on the optical signal (Figure 5b). At faster scan rates, the analyte had less time to be electrolyzed. Correspondingly, the maximum absorbance change decreased from 0.066 at 2.0 mV/s to 0.038 at 500 mV/s. A plot of ΔA is shown in Figure 5b (triangles) and is nonlinear with the square root of the scan rate. The nonlinearity can be traced to the large contribution of ITO to ΔA, in addition to the ΔA for ferricyanide. The total absorbance change on electromodulation at each concentration, $\Delta A_{total,}$ is the sum of the analyte contribution, ΔA_{ferri}, and that of ITO, ΔA_{ITO}

$$\Delta A_{total} = \Delta A_{ferri} + \Delta A_{ITO} \quad (4)$$

where the ΔA values are obtained from the absorbance extremes

(48) Petit-Dominguez, M. D.; Shen, H.; Heineman, W. R.; Seliskar, C. J. *Anal. Chem*. **1997**, *69*, 703−710.
(49) Maizels, M.; Seliskar, C. J.; Heineman, W. R. *Electroanalysis* **2000**, *12*, 241−247.

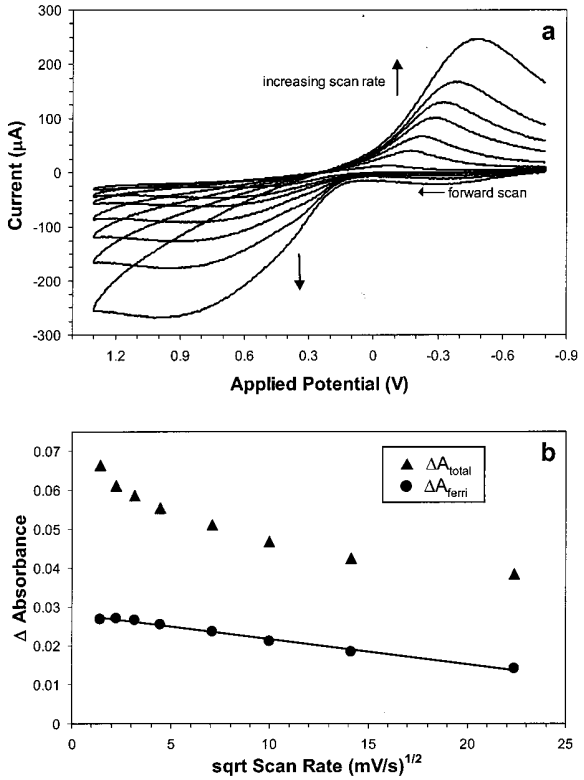

Figure 5. Scan rate study with a PDMDAAC−SiO_2 coated ITO IEBK7 sensor. The sensor was preequilibrated with 5 mM $Fe(CN)_6^{4-}$ in 0.1 M KNO_3 for 1 h. The potential was scanned between −0.80 and +1.30 V at scan rates of 2.0, 5.0, 10, 20, 50, 100, 200, and 500 mV/s. (a) Cyclic voltammograms in order of increasing scan rates from the zero current line. *E* (V) vs Ag/AgCl. (b) Optical responses of ΔA_{total} (the change in absorbance of the waveguide preloaded with $Fe(CN)_6^{4-}$ in 0.1 M KNO_3) and of calculated ΔA_{ferri}. The solid line was calculated using linear regression with $R^2 = 0.990$; $\lambda = 442$ nm.

in the potential step scan for the analyte-loaded sensor (ΔA_{total}) and the sensor in supporting electrolyte (ΔA_{ITO}). After accounting for the contribution of ITO, the ΔA_{ferri} values (Figure 5b, circles) were found to be linear with $\sqrt{v}$, agreeing with the results obtained for the peak current versus $\sqrt{v}$. Thus, the electrochemistry and the optical modulation of the analyte faithfully report the same results.

All of the CVs in Figure 5a depart from ideal $Fe(CN)_6^{3-/4-}$ behavior. The distortions, especially the potential peak separation (ΔE_p) and the CV asymmetry, have been attributed to the high resistance of the ITO electrode and to a slow heterogeneous electron transfer rate constant, *k*. With many of our ITO films with resistances approaching 1 kΩ, measured peak separations were as high as 1400 mV at the fastest scan rate. The large *iR* drop would be more pronounced because of higher currents from preconcentration of the analyte by the selective film.[4] These peak separations are consistent with those (1240 mV) measured by Martinez[40] with a 203 Ω/□ bare ITO electrode and 10 mM $Fe(CN)_6^{4-}$ at 200 mV/s. In addition to an *iR* drop, a slow heterogeneous electron-transfer *k* would contribute to potential peak separation.[4,40] Practically, the nonideal electrochemical behavior requires a larger than anticipated potential range to sufficiently electrolyze the analyte during electromodulation. This range extension, in turn, increased the ΔA_{ITO} blank response.

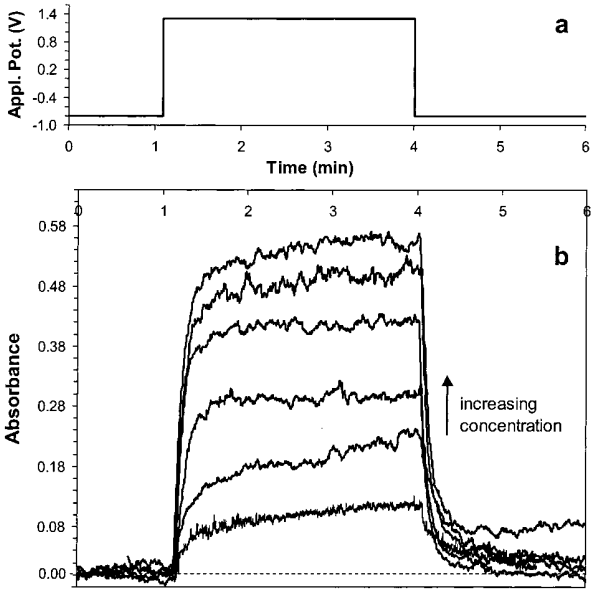

Figure 6. Electromodulation of $Fe(CN)_6^{4-}$ in 0.1 M KNO_3 with a PDMDAAC−SiO_2-coated ITO IEBK7 sensor. (a) The excitation potential waveform applied with all concentrations. (b) Optical response to different concentrations of $Fe(CN)_6^{4-}$ from bottom to top: 0.00, 0.10, 0.50, 1.0, 5.0, and 10 mM. *E* (V) vs Ag/AgCl; λ = 442 nm.

Finally, a goal in the development of the waveguide sensor was to demonstrate its use for quantification of ferrocyanide. Spectroelectrochemical modulation using the potential step waveform in Figure 6a gave the results for $Fe(CN)_6^{4-}$ concentrations ranging from 0.10 to 10 mM shown in Figure 6b. The optical signals rose quickly after the potential was stepped to +1.30 V and decreased quickly for the reverse step, indicating that the analyte was efficiently electrolyzed in the film. The large background response for pure supporting electrolyte (bottom-most curve, Figure 6b) exerts a major influence on the results. The optical signal for the forward step does not plateau as expected for complete electrolysis of analyte in the optical cell of the film because of the blank response. Also, the magnitude of ΔA_{ITO} prevents lower concentrations from being measured. The optical background could be reduced by narrowing the potential step limits from the presently chosen values, but this would reduce the rate of electrolysis of the analyte because of the large *iR* drop.

In the calibration curve plotted in Figure 7, the ΔA_{ferri} values were calculated from eq 4. The shape of the calibration curve is nearly identical to calibration curves for comparable systems with spectroelectrochemical MIR sensors.[1,4,7] The linear portion of the curve is at the lower concentrations, and the ΔA_{ferri} values then level off at the higher concentrations as the ion-exchanging film becomes saturated.

The sensitivity ($\Delta A/\Delta[Fe(CN)_6^{4-}]$) was ~6 times greater with this waveguide sensor than with an analogous MIR sensor[51] ($\Delta A_{ferri} = 0.048$ with the MIR device; $\Delta A_{ferri} = 0.31$ with the waveguide). Thus, even though the limit of detection is restricted

(50) Ramos, B. L.; Choquette, S. J.; Fell, Jr., N. F.; *Anal. Chem.* **1996**, *68*, 1245−1249.
(51) Stegemiller, M. L., unpublished results.

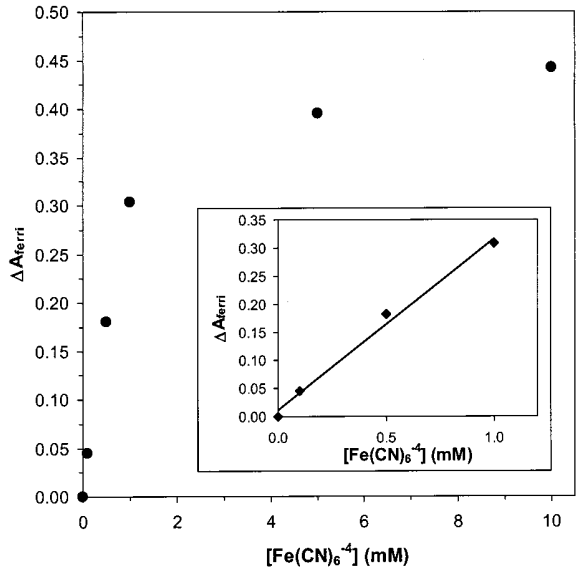

Figure 7. Calibration curve for optical detection of $Fe(CN)_6^{4-}$ in 0.1 M KNO_3 with a PDMDAAC−SiO_2-coated ITO IEBK7 sensor generated by potential step modulation (see previous figure). The inset shows the linear region ($R^2 = 0.991$) of the curve; $\lambda = 442$ nm.

by the large blank signal, an increased sensitivity is found relative to the MIR device.

CONCLUSIONS

A spectroelectrochemical sensor based on planar waveguide technology has been fabricated and with it electromodulation of an analyte has been demonstrated. Overall attenuation losses within the sensor were large due to the layering of ITO directly onto the waveguide and to inefficient (prism) coupling. The losses due to ITO may be attributed to a significant free carrier absorption within the semiconductor. The high electrical resistance of the ITO layer was accompanied by significant changes in its optical properties during electromodulation over the potential range of the analyte, ferrocyanide. Nonetheless, the contribution of ITO is linear with applied potential and can be quantitatively subtracted from the overall optical modulation signal yielding an adequate calibration curve for the analyte. Despite the associated relatively high detection limit, this prototype waveguide spectroelectrochemical sensor yields a moderate improvement of ∼6× in sensitivity over the corresponding MIR device.

To obtain better sensitivity and detection limits, improvements in the prototype waveguide need to be made. These might include the following: direct fiber coupling to the waveguide or grating coupling[50] as a replacement for prism coupling; optimization of the ITO layer (thickness and resistance) and possibly its isolation from the waveguide layer by insertion of a silica buffer layer; optimization of the chemically selective film[5,7,22] (thickness and polyelectrolyte concentration) to maximize analyte uptake and preconcentration.

ACKNOWLEDGMENT

We thank Prof. F. J. Boerio for use of the ellipsometer, Imants Zudans for performing the ellipsometry experiments, and Prof. T. H. Ridgway for many helpful discussions. This work was supported by a grant awarded by the Environmental Management Sciences Program of the U.S. Department of Energy, Office of Environmental Management (Grant DE-FG0796ER62311), and by a Procter & Gamble Fellowship (S.E.R.).

Received for review July 6, 2000. Accepted September 11, 2000.

AC0007736